Research Article

Anne Kauter, Silvio Bürge, Christian Klotz and Michael Laue*

Serial block-face scanning electron microscopy of adherent cells on thin plastic substrate

https://doi.org/10.1515/mim-2024-0007
Received March 31, 2024; accepted May 24, 2024;
published online June 25, 2024

Abstract: Serial block-face (SBF) scanning electron microscopy (SEM) is used for imaging the entire internal ultrastructure of cells, tissue samples or small organisms. Here, we present a workflow for SBF SEM of adherent cells, such as *Giardia* parasites and HeLa cells, attached to the surface of a plastic culture dish, which preserves the interface between cells and plastic substrate. Cells were embedded *in situ* on their substrate using silicone microwells and were mounted for cross-sectioning which allowed SBF imaging of large volumes and many cells. A standard sample preparation and embedding protocol for thin section electron microscopy provided already sufficient resolution and image quality to visualize larger structures. To improve resolution and image quality of SBF imaging, we stepwise tested modifications of the protocol, such as the moderate increase of the heavy metal content of the sample. Modifications of the embedding by either the reduction of the resin layer (minimal embedding) or the addition of silver colloid to the resin were evaluated at high and low vacuum imaging conditions. The optimized sample preparation protocol is very similar to the standard preparation protocol for thin section electron microscopy, so that the samples can also be used for this application. The protocol applies a higher concentration of osmium tetroxide, a higher temperature for heavy metal incubation and an additional lead *en bloc* staining. In summary, the presented workflow provides a generic and adaptable solution for studying adherent cells by SBF SEM.

***Corresponding author: Michael Laue**, Advanced Light and Electron Microscopy (ZBS 4), Centre for Biological Threats and Special Pathogens, Robert Koch Institute, Seestraße 10, D-13353 Berlin, Germany,
E-mail: lauem@rki.de. https://orcid.org/0000-0002-6474-9139
Anne Kauter and Silvio Bürge, Advanced Light and Electron Microscopy (ZBS 4), Centre for Biological Threats and Special Pathogens, Robert Koch Institute, Seestraße 10, D-13353 Berlin, Germany
Christian Klotz, Mycotic and Parasitic Agents and Mycobacteria (FG16), Department of Infectious Diseases, Robert Koch Institute, D-13353 Berlin, Germany

Keywords: cell culture; *Giardia lamblia*; HeLa cells; transmission electron microscopy; scanning electron microscopy; volume imaging

1 Introduction

Serial block-face (SBF) scanning electron microscopy (EM) is one of the imaging methods to study large volumes (i.e. entire cells or small tissue samples) of biological samples by EM (see [1] for an overview about the various techniques). It uses an ultramicrotome built into the chamber of a scanning electron microscope for automated alternate sectioning and imaging of the block-face [2]. Imaging is usually performed with detectors that collect the backscattered electrons reflected from a thin volume below the flat block-face during scanning with the primary electron beam. To generate sufficient backscattered electrons for obtaining suitable resolution and contrast, the method requires that heavy metals or other atoms with a larger size are selectively deposited in the samples during preparation. Popular strategies apply reduced osmium tetroxide with additional enhancer steps, as the application of thiocarbohydrazide, additional osmium tetroxide incubation and *en bloc* contrasting with uranyl acetate and lead citrate (e.g. [3]), which mainly increase the membrane contrast. The heavy metal deposition not only increases the signal and contrast for imaging, but also sample conductivity [4] which is important because the resin embedded samples are usually good insulators that charge easily during scanning with the electron beam. To improve sample conductivity further, different additional strategies were applied. One strategy is to reduce the amount of non-conductive resin around the object (minimal resin embedding; e.g. [5]) or the addition of conductive material, such as silver colloid ([6], page 122) or carbon/Ketjen black [7], to the resin. Other strategies apply ionized gas, either by using low vacuum in the entire sample chamber [2] or local gas injection [8], or a positive biased grounding of the sample [9] to compensate the charging of the sample block. As a consequence, various sample preparation and imaging work flows are already available in the

literature but usually needed to be adapted further to fit the variety of biological objects and scientific questions.

Adherent cells cultured on solid supports, such as glass or plastic, are an important class of samples, because they are widely used in the life sciences. For SBF SEM, cell layers are usually removed after the sample preparation to allow ultrathin sectioning. In experiments with infectious pathogens, plastic dishes or multi-well plates are preferred over glass, because glass may damage personal protection or, in case of a disaster, is more difficult to handle if broken. For high quality imaging with light and laser microscopes, dishes, slides and multi-well plates with a thin plastic bottom were introduced and widely used, also for correlative light and electron microscopy (e.g. [10]). An advantage of the thin plastic bottom, besides its optical properties, is that it can be sectioned by ultramicrotomy [11], [12]. Here, we present a method which allows the use of culture dishes with a thin plastic bottom for adherent cell cultivation, embedding *in situ* and direct cross-sectioning without the removal of the plastic bottom. Besides classical thin sectioning for transmission EM, the protocol allows SBF SEM of large volume and area to collect data from many cells present in a sample block. This was particular useful for the characterization of mutant phenotypes of the parasite *Giardia lamblia*. We further demonstrate, by using HeLa cells, that, with only slight modification of the standard post-fixation and embedding protocol for transmission EM, the resolution and image quality of SBF SEM could be improved.

2 Materials and methods

2.1 Cell culture and fixation of *G. lamblia* and HeLa cells

G. lamblia (synonymous *Giardia intestinalis* or *Giardia duodenalis*) trophozoites (strain WBC6, ATCC 50803) were grown at 37 °C without shaking in modified TYI-S-33 medium [13] supplemented with bovine bile, 10 % adult bovine serum. After reaching confluence, cells were incubated on ice for 30 min to detach them from the walls of the cultivation vial. The suspension with detached *Giardia* trophozoites was added to warmed medium and seeded in inserts of a plastic dish (Culture-inserts 2 Well in 35 mm µ-Dish, ibiTreat, ibidi, No. 81176) and cultivated up to 90 % confluence at 37 °C under anaerobic conditions using AneroGen jars and appropriate reaction bags (Oxoid, No. AN0025) as previously described [14].

HeLa cells (ATCC CCK 2) were cultivated in DMEM high glucose (Gibco, No. 41965039) including 10 % fetal bovine serum (Sigma-Aldrich, No. F7524). For the block-face imaging experiments, plastic cell culture dishes (micro-Insert 4 well in 35 mm µ-Dish, ibiTreat, ibidi, No. 80406) with four micro inserts (1.5 × 2 mm, 10 µl volume) were used. Optionally, dishes were coated with 10 nm of gold-palladium (Au/Pd) using a sputter coater (E5100 Series II, Polaron) (see results for more information). Before seeding, the plastic surface was treated with collagen (Collagen Type I, rat tail; ibidi, No. 50203) at a concentration of 115 mg/ml in 0.1 % acetic acid for 1 h. After three washes with phosphate-buffered saline, dishes were dried. HeLa cells were seeded at a concentration of 2×10^5 cells/ml and 10 µl per well and cultivated for 12–18 h at 37 °C and 5 % carbon dioxide.

Cells were chemically fixed by removing the culture medium and by adding the fixation solution, which was comprised of 2.5 % glutaraldehyde in 0.05 M Hepes buffer, supplemented with glucose and salts (1 g/l glucose, 8 g/l NaCl, 0.4 g/l KCl, 98 mg/l $MgSO_4$, 185 mg/l $CaCl_2 \times 2H_2O$). Incubation with the fixative was performed at room temperature for at least 2 h. Finally, dishes with fixed cells were stored at 8–10 °C until further processing.

2.2 Post-fixation and resin embedding

2.2.1 Standard protocol for thin section electron microscopy

Giardia cells were processed *in situ* using the silicone dish inserts as containers for post-processing and embedding. The applied protocol generally is used as a standard for studying especially virus-cell interactions [15] and is provided as a step-by-step protocol in the Supplementary Material. Briefly, cells were post-fixed with 1 % osmium tetroxide in water (1 h), followed by 0.2 % tannic acid in 0.05 M Hepes buffer (1 h) and, as variant of the original protocol, a 1:1 mixture of 2 % uranyl acetate and UA-Zero EM Stain (Agar Scientific) (1 h). Dehydration was performed in an ascending series of ethanol. Cells were infiltrated with Epon (medium hardiness, see step-by-step protocol in Supplementary Material) using mixtures of acetone and Epon (1:1, followed by 1:2, for 1 h each and by 1:3, overnight), before they were embedded in pure Epon and polymerized at 60 °C.

2.2.2 Modified protocol for serial block-face scanning electron microscopy

The modified embedding protocol for serial block-face scanning (SBF) electron microscopy (SEM) was tested and optimized using HeLa cells. It was performed in two days (see Supplementary Material for a step-by-step protocol).

Day one ends with uranyl acetate incubation at 8–10 °C, overnight (18–20 h). On the second day the samples were brought to 60 °C in an oven on an aluminum block for fast heat transfer and incubated for another hour. Dehydration was done with an ascending series of ethanol. Infiltration with Epon was conducted with acetone/Epon mixtures (see Supplementary Material for details and below for minimal resin embedding). The Epon mixture was adjusted to provide harder blocks (Epon hard mixture) than in the standard protocol (see Supplementary Material for the precise composition of the mixture) and, finally, was polymerized at 60 °C for at least 24 h.

2.2.3 Modifications of the heavy metal treatment

(1) Increased concentration of osmium tetroxide and incubation temperature – The osmium tetroxide concentration was increased to 4 % and the processing temperature for osmium tetroxide, tannic acid and uranyl acetate was set to 60 °C. For incubation at 60 °C, dishes were placed in an oven on an aluminum block for fast heat transfer.
(2) Addition of lead *en bloc* staining – After the uranyl acetate *en bloc* staining, lead aspartate according to Walton [16] was applied for 30 min at 60 °C in an oven on an aluminum block for fast heat transfer.
(3) Addition of a second osmium tetroxide incubation step – After tannic acid treatment and before the uranyl acetate *en bloc* staining, a second osmium tetroxide incubation step was added to the protocol. The concentration was set to 4 % in water and incubation time was 1 h at 60 °C in an oven on an aluminum block for fast heat transfer.

2.2.4 Minimal resin embedding

Two variants of minimal resin embedding were tested. In both variants, the culture inserts were removed at the end of the last infiltration step (i.e. 3:1 mixture of Epon and acetone for 1 h) and polymerization was subsequently performed at 60 °C. In the first variant, the acetone/Epon mixture was removed with a positive displacement pipette down to a thin remaining layer before the culture insert was removed. In the second variant, the thin layer was further thinned by blowing away the acetone/Epon mixture with pressurized air (Dust-Off Plus, Falcon) from the side ([17], pages 164–165) after removal of the inserts. A step-by-step description of the protocol is documented in the Supplementary Material.

2.2.5 Silver colloid resin embedding

As additional modification, the Epon was supplemented with silver colloids to improve conductivity ([6], page 122). The Epon (hard mixture) was freshly prepared for each experiment to minimize viscosity. Frozen/thawed mixtures increase in viscosity which interferes with the uniform distribution of silver in the Epon. For every experiment, a stock mixture of Epon and acetone (3 + 1 volume units), supplemented with silver colloid (Sigma-Aldrich, No. 484059), was produced. The colloid concentration was empirically set to a 10th of the numerical volume of the Epon (e.g. 0.45 g silver colloid in 4.5 ml Epon plus 1.5 ml acetone). For infiltration, the stock mixture was diluted with acetone to achieve mixtures of 2 + 1 and 1 + 1 volume units of Epon and acetone with reduced silver colloid concentration. The mixtures were prepared for each dish in a separate reaction vial and mixed for at least 10 min by using a 3D lab mixer for vials. Before use, the mixtures were placed in an ultrasonic incubator (Sonorex Super 10P, Bandelin) for 10 min at maximum power. Embedding was performed as minimal embedding, which is described above. Note, that it is also possible to conduct the polymerization of the sample without removing the inserts as in the minimal resin embedding approach, which usually produced a gradient of silver distribution in the final block with highest concentration at the bottom.

2.3 Sample mounting and conventional thin sectioning

Polymerized samples were extracted from the dish by using a hot scalpel blade (Supplementary Figure 1C) and separated from each other. If the inserts were not removed during the embedding process, they were carefully peeled of the individual samples by cutting first the corners of the silicone wells with a hot scalpel or sharp razor blade. While the samples prepared according to the minimal resin embedding protocol could be directly used for mounting at 90° after sample extraction, normally filled inserts were flattened on one side by using a jigsaw and/or a razor blade and, optionally, reduced in length and height. Finally, samples were mounted on stubs for serial-block face imaging (Micro to Nano, No. 10-006009-50) by using conductive glue (MG Chemicals, No. 8331S, provided by Micro to Nano, No. 15-002433) (Supplementary Figure 1D).

Mounted samples were shortened to roughly 1.5 mm height and laterally trimmed using a razor blade. Then,

samples were polished and trimmed with an ultramicrotome (UC7, Leica Microsystems). First, a diamond knife (histo cryo 45°, Diatome) was used to produce a flat block face (Supplementary Figure 1E). Second, the block-face for serial-block face imaging was trimmed with a trimming diamond (trim 90, Diatome) to a size of $1000 \times 250 \times 250$ µm ($l \times w \times h$) (Supplementary Figure 1F) and with the cell layer oriented in the middle of the block-face (Supplementary Figure 2). Finally, the sample was coated with 10 nm of Au/Pd in a sputter coater (E5100 Series II, Polaron) and polished again using a diamond knife (ultra 45°, Diatome) with low sectioning speed (1 mm/s) and a section thickness (below 100 nm).

Thin sections for transmission electron microscopy were taken from the samples either after the first block-face polishing or from the final block trimmed for serial-block face imaging using the ultramicrotome and a diamond knife (ultra 45°, Diatome). The sections were between 60 and 70 nm in thickness and collected on naked copper grids (300×75 mesh). To achieve more contrast, sections were optionally stained with 2 % uranyl acetate and 0.1 % lead citrate. Finally, sections were coated with a thin layer of carbon to obtain more stability during imaging.

2.4 Transmission electron microscopy

Imaging of thin sections was performed with a transmission electron microscope (Tecnai Spirit, ThermoFisher) operated at 120 kV. Images were recorded with a side-mounted CMOS camera (Phurona, EMSIS) at 4112×3008 pixel (16 bit). For presentation in the figures, images were converted to 8 bit and adjusted for brightness and contrast using Photoshop (Adobe).

2.5 Serial block-face scanning electron microscopy

Block-face imaging and serial sectioning were done with a field-emission scanning electron microscope (Teneo Volumescope, ThermoFisher) that was equipped with an ultramicrotome. The microscope was operated either at high vacuum, using the in-lens back-scattered electron detector (T1) with a ring filter mounted at the final lens, or at low vacuum, using the Volumescope directional backscatter electron detector (DBS). The low vacuum mode is achieved by a controlled supply of water vapor (0.3–0.5 mbar) to the sample chamber of the microscope. The water vapor molecules were ionized during imaging by the electrons and compensate charging of the sample blocks introduced by the primary electron beam.

2.5.1 Serial block face scanning electron microscopy of Giardia cells prepared with the standard protocol for thin section electron microscopy

Mounted and trimmed samples were inserted in the microtome of the Volumescope and adjusted as described in the manual. Imaging and sectioning were performed at low vacuum with the DBS detector and setting the water vapor pressure to 0.5 mbar. Imaging at lower pressure resulted in charging or irregular sectioning. The entire block-face was initially scanned for an overview image and up to 10 frames were distributed across the surface of the block-face for imaging (see Supplementary Figure 3). During sectioning, the operator checked whether the frames included cells or not and removed or placed frames on the block-face. Frames were scanned at 4 or 5 nm pixel size with 6144 by 4096 pixels (16 bit) and a dwell time of 1 µs per pixel at 2 kV and 0.1 nA. Section thickness was either set to 50 nm (4–5 nm pixel size) or 10 nm (5 nm pixel size).

Post-processing of the image stacks was performed with Fiji [18] and Microscopy Image Browser (MIB, Version 2.84, [19]) (see Supplementary Material for a detailed list of the applied algorithms and parameter). Stacks were cropped to the cell of interest and aligned using the StackReg Plugin (translation) of Fiji. Smoothing was performed with the FeatureJ Plugin (Derivatives, smoothing scale = 0.9) of Fiji. After reducing the images to 8 bit, the lookup table was inverted and contrast homogenization was performed by either using Fiji and the integral image filter “Normalize local contrast” (setting the block radius to the entire image), or using MIB and the contrast homogenization function with setting the reference to the dish bottom or extracellular background. Optionally, images were scaled by a factor of 0.5 (bilinear interpolation) and filtered with an FFT-bandpass filter (40, 3 nm) using Fiji to highlight the ventral disc structures of the parasite. See Supplementary Figure 4 for a series of images demonstrating the results of the image processing.

Segmentation of cells, nuclei and ventral disc microtubule structures was done with MIB. Cells were segmented by using the semi-automatic graph-cut algorithm. Nuclei and disc microtubule structures were manually labelled on some of the images and completely labelled by using the interpolation function of MIB. Exported labels were checked in Fiji and manually corrected if they were incomplete or irregular. Cell and nuclei labels were filtered in Fiji with a median filter (2 pixels). For modeling, labels were imported in Imaris (10.0, Oxford Instruments) and surface rendering was performed using the “create surface” wizard

setting the surface resolution to 0.06 µm and a slight correction of the automated threshold detection. Video animation of the model was generated with the Imaris animation tools. Videos of the image series were produced by screen recording of animated series in Fiji using Claquette (3.03., Peakstep).

2.5.2 Serial block face scanning electron microscopy of HeLa cells prepared with the modified protocols

To check which imaging parameters were suitable to achieve stable SBF imaging of samples prepared with the modified embedding protocols, imaging parameters were set to following values or varied in the following range: acceleration voltage was set to 2 kV with a current between 0.1 nA and 0.05 nA; scan range was set to 3077×2048 or 6144×4096 pixel; dwell time was 0.5 or 1 µs with or without a line integration of 2.; for imaging at low vacuum, water vapor pressure was set between 0.3 and 0.45 mbar. Maximum achievable pixel resolution was determined empirically for a section thickness of 50 and 10 nm by reducing the pixel size stepwise, tuning the imaging conditions, such as beam current, dwell time per pixel in the range defined above, and evaluating the visibility of ultrastructures. Post-processing of image stacks and recording of the videos of the animated image series were performed as described above (see also Supplementary Material).

3 Results

The starting point of the present study was a project on the enteric parasite *G. lamblia*, in which the phenotype of various mutations of ventral disc proteins was analyzed [20], [21]. The parasite uses the ventral disc for adhesion to the host duodenal epithelium and, therefore, is an essential factor of pathogenicity [22]. The main target structure of the analysis was the complex and spiral-formed microtubule apparatus which shapes the ventral disc [23]. We started with conventional thin sectioning of the parasites cultivated on thin plastic bottom of plastic culture dishes which revealed ultrastructural detail at high resolution (Figure 1A and B). The complexity of the observed phenotypes prompted us to consider volume imaging for a more comprehensive analysis of the ventral disc morphology. Instead of performing an additional cultivation and particular processing for volume imaging, we tested, if the already available sample blocks, prepared with a standard thin section embedding protocol (osmium tetroxide, tannic acid, uranyl acetate/UA-Zero, Epon), were suitable for serial block-face (SBF) scanning electron microscopy (SEM) at sufficient resolution. To our surprise, the resulting data sets were of sufficient quality to reconstruct the entire ventral disc microtubule apparatus in 3D (Figure 1C and D). The SBF SEM of cross-sections through the adherent parasite allowed us to collect complete volumes of many cells with a section thickness down to 10 nm (Supplementary Videos 1 and 2). Most remarkable, the dish bottom did not interfere with the serial sectioning and the interface between cells and substrate was preserved (Figure 1C).

While the results were sufficient to reveal the gross morphology of the ventral disc microtubule apparatus, the structural resolution and contrast was limited. Besides the comparatively moderate heavy metal staining provided by our standard protocol (osmium tetroxide, tannic acid, uranyl acetate/UA-Zero), that generates only few back-scattered electrons and, thus, low contrast, we needed to operate the microscope at low-vacuum conditions (i.e. 0.5 mbar; water vapor) to prevent charging, which both limit the resolution of SBF SEM (see also discussion). To find out, what we need to achieve a better resolution, we started experiments with HeLa cells cultivated in plastic dishes equipped with small silicone inserts (2×1.5 mm). In a series of experiments, we tried to improve both, electrical conductivity and contrast of the samples to achieve better resolution and image quality for SBF SEM of cells attached to plastic surface. To improve electrical conductivity, we finally studied the following modifications of the basic protocol: (1) slight increase of heavy metal deposition by increasing temperature and concentration of the osmium tetroxide incubation; (2) addition of a thin conductive metal layer on the bottom surface of the plastic dish; (3) addition of silver colloid to the Epon resin; (4) reducing the layer of resin on top of the cells (minimal resin embedding) in two variants (first, removal of inserts and, second, additional reduction by blowing with pressurized air).

To compare the effects of the different modifications of the protocol, we trimmed the sample blocks to the same size and shape ($1 \times 0.25 \times 0.25$ mm) and set the imaging conditions to fixed parameters (3072×2048 pixels, 1 µs dwell time, 0.1 nA, 2 kV, lookup table = inverse). Imaging was performed at high vacuum, using a backscattered-electron detector (T1) localized in the final lens with ring-filter mounted to the lens, and at low vacuum (set to 0.3 mbar water vapor) using the Volumescope directional backscattered electron (DBS) detector. We qualitatively evaluated the imaging at increasing magnification (i.e. lower pixel size) with regard to distortions introduced by charging and compared the limit of resolution/visibility of cellular structures achieved with the different protocols. The imaging result

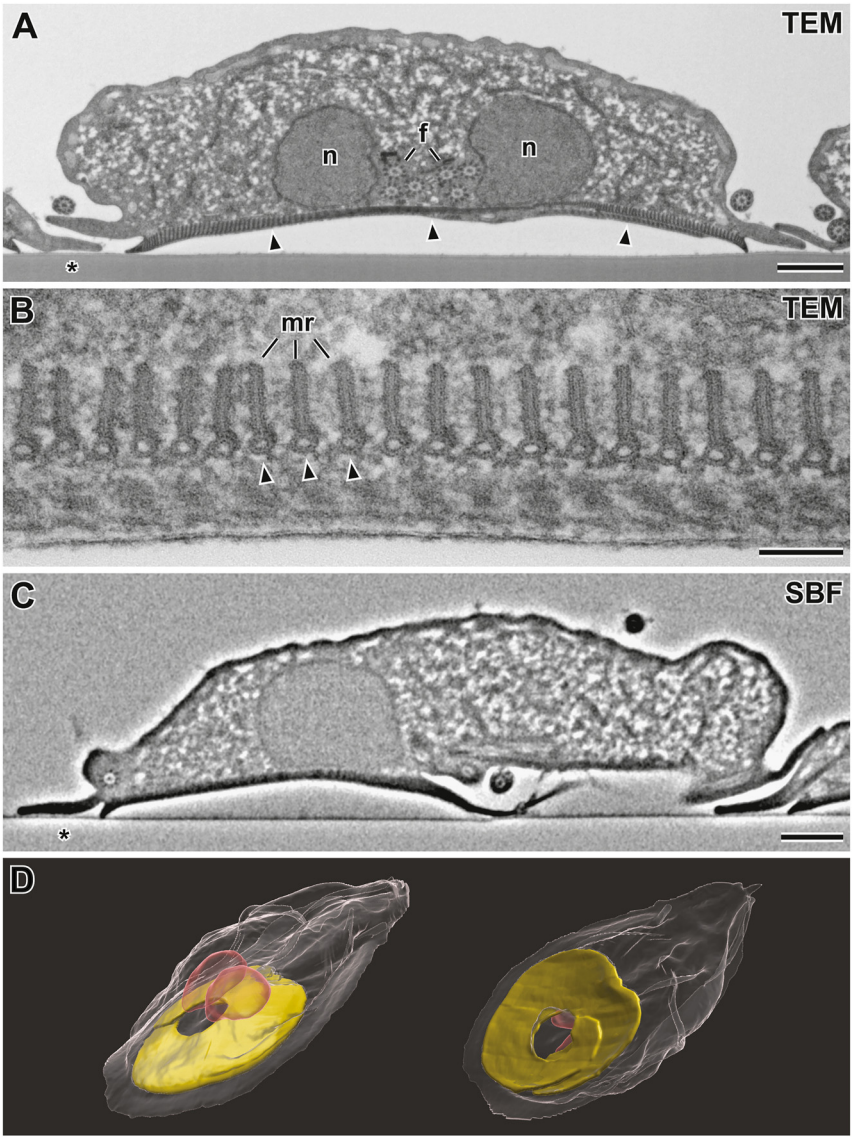

Figure 1: Ventral disc of *Giardia lamblia.* (A and B) Transmission electron microscopy (*TEM*) of thin cross-sections through *Giardia* cells adherent to the plastic bottom of a culture dish (*). (A) Profile of an entire cell with the two nuclei (*n*), flagellar axonemes (*f*) and ventral disc (*arrowheads*). (B) Detail of the microtubule apparatus forming the ventral disc. The microtubules (*arrowheads*) are registered in parallel and connected to band-like micro-ribbons (*mr*). (C) Serial block-face scanning electron microscopy (*SBF*) of an adherent *Giardia* cell. A single image of one section is shown from a series of 276 sections (see Supplementary Video 1 for the entire series). (D) Two screen shots of a model reconstructed from the image series (ventral disc in yellow, nuclei in red). See also Supplementary Video 3 for a rotational animation of the model. Scale bar in A and C = 1 µm, B = 100 nm.

was insufficient if charging already distorted the cells or cellular ultrastructures at a resolution above 20 nm pixel size. Resolution and image quality (mostly noisiness) affect the visibility of small or thin subcellular structures, such as the endoplasmic reticulum or small vesicles. Here, we define a low resolution and image quality if the cellular ultrastructures were detectable at a resolution down to 10 nm without any distortions by charging. Higher resolution and image quality is achieved with either lesser noise and/or better resolution (i.e. a pixel size below 10 nm).

Increase of osmium tetroxide concentration (from 1 to 4 %) and incubation temperature (from room temperature to 60 °C) for the entire post-fixation procedure (osmium tetroxide, tannic acid, uranyl acetate) already provided sufficient contrast and thus visibility of structures for imaging at low vacuum (Table 1, protocol 01; Figure 2A). Imaging at high vacuum with these samples was only possible after addition of silver colloids to the Epon (protocol 03 to 06; Table 1; Figure 2C) but still produced visible charging. Interestingly, the addition of silver did not improve the imaging

Table 1: Resolution and image quality of block-face imaging of HeLa-cells after sample preparation with increased heavy metal content and modified embedding.

Protocol ID	Cell treatment	Embedding	Au/Pd coating	Resolution & image quality	
				High vacuum T1	Low vacuum DBS
01	4 % Os 0.2 % TA 2 % UA 60 °C	Epon	−	o	•
02	4 % Os 0.2 % TA 2 % UA 60 °C	Epon, minimal (air blow)	−	o	•
03	4 % Os 0.2 % TA 2 % UA 60 °C	Epon, silver, minimal (air blow)	−	•	•
04	4 % Os 0.2 % TA 2 % UA 60 °C	Epon, silver, minimal (air blow)	+	•	•
05	4 % Os 0.2 % TA 2 % UA 60 °C	Epon, silver, minimal	−	•	•
06	4 % Os 0.2 % TA 2 % UA 60 °C	Epon, silver, minimal	+	•	•
07	4 % Os 0.2 % TA 2 % UA Pb 60 °C	Epon, silver, minimal (air blow)	+	••	••
08	4 % Os 0.2 % TA 2 % UA Pb 60 °C	Epon, minimal (air blow)	+	•	••
09	4 % Os 0.2 % TA 4 % Os 2 % UA Pb 60 °C	Epon, silver, minimal (air blow)	+	••	••
10	4 % Os 0.2 % TA 4 % Os 2 % UA Pb 60 °C	Epon, minimal	+	••	••
11	4 % Os 0.2 % TA 4 % Os 2 % UA Pb 60 °C	Epon, minimal	−	••	••
		Insufficient			o
		Low			•
		Higher/better			••

of these samples at low vacuum (compare protocol 01 and 02 with protocol 03 to 06, Table 1). In contrast, local charging was observed at imaging conditions under low vacuum which revealed no charging in samples without the addition of silver to the Epon (compare Figure 2A with 2B).

The addition of a conductive metal coating at the bottom of the dish (Supplementary Figure 1) and the mode of the minimal embedding had no significant effect on the maximal achievable imaging quality and resolution (Table 1). The thin metal coating of the dish bottom was introduced to the protocol because at a high cell confluence (>90 %) the plastic bottom tended to split unevenly from the cells during sample extraction, mounting or trimming. With the metal coating in place, the bottom occasionally separated from the cells, but the remaining surface below the cells was smooth and not uneven like in samples in which the metal coating was lacking. The occasional split of the dish bottom from the embedded cells had no influence on the sectioning and image quality.

To further increase the resolution and image quality of the block-face imaging, we sequentially added more heavy metals to the sample during preparation. In the exploratory phase of our project, we tested whether reduced osmium tetroxide and repeated osmium tetroxide application, optionally with thiocarbohydrazide (TCH) as enhancer, will increase resolution and image quality of the SBF imaging or not. The reduced osmium tetroxide post-fixation with potassium ferrocyanide resulted in a significant loss of cells during incubation and was not considered further. We noted this effect also in other projects in which we applied the reduced osmium tetroxide/TCH/osmium tetroxide protocol introduced by Deerinck et al. [3] on HeLa cells adhered to the glass bottom of a culture dish (35 mm without inserts). The application of TCH to cells cultured in silicone micro-wells resulted in the formation of larger dense precipitates, inhomogeneous heavy metal staining of the cells and was also not further considered. We tested two principal modifications of our protocol with increased osmium tetroxide concentration and high temperature of incubation (protocol 01): (1) Addition of a lead aspartate *en bloc* contrasting according to Walton [16] and (2) addition of a second osmium tetroxide incubation, after tannic acid and before uranyl acetate treatment, followed by lead aspartate *en bloc* contrasting. Both modifications were tested using minimal embedding with or without the addition of silver colloid (Table 1, protocol 07 to 11).

The addition of further incubation steps with heavy metals to the sample preparation resulted in improved resolution and image quality in block-face imaging (Table 1, protocol 07 to 11). The addition of silver colloid improved only the imaging at high vacuum (Table 1, protocol 07 and 08) with less significance at highest heavy metal load tested (Table 1, protocol 09 to 11). The contrast of the samples which were prepared with a single osmium tetroxide incubation and an additional *en bloc* treatment with lead aspartate allowed a proper discrimination of the main organelles and cytoplasmic structures already at low magnification (Figure 3A and B). The appearance of cells was very similar to the appearance of cells in thin sections taken from

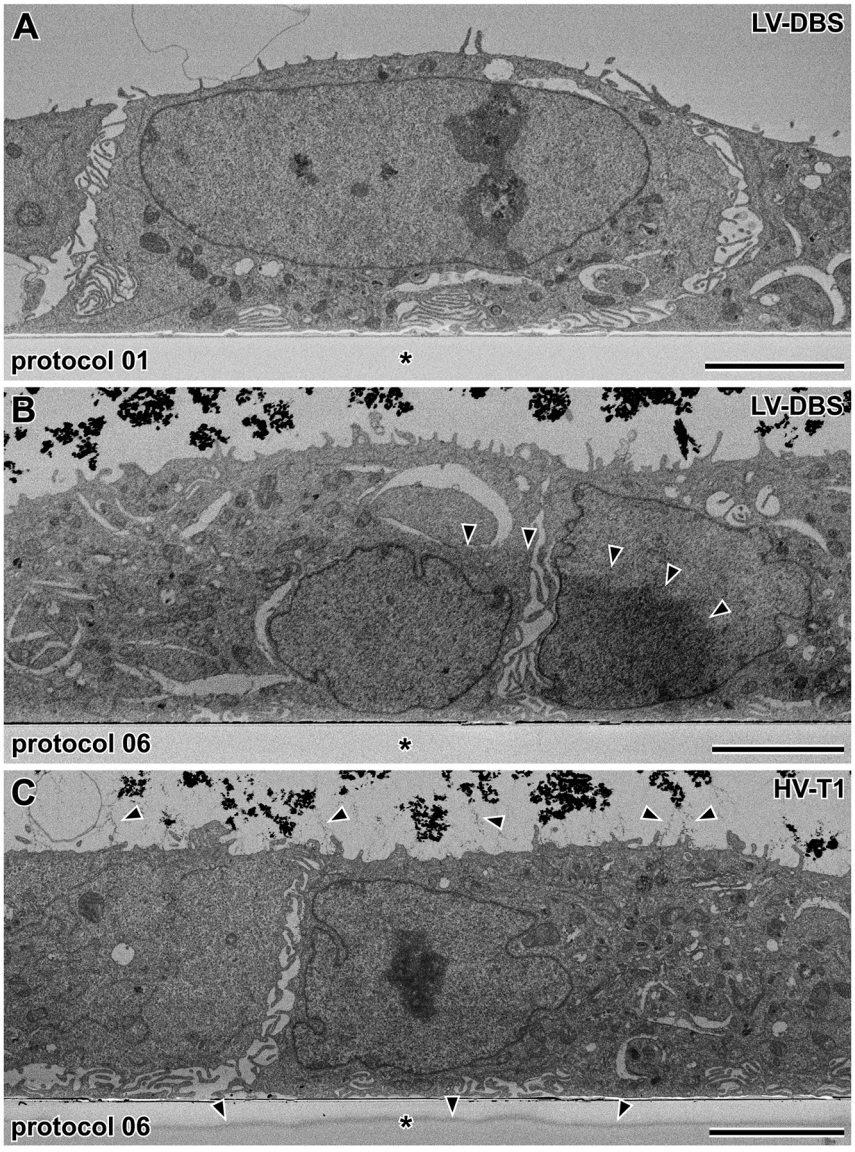

Figure 2: Block-face SEM of adherent HeLa cells in cross-section prepared with different protocols to increase conductivity. (A) Increased osmium tetroxide concentration and temperature of post-fixation (60 °C, protocol 01, Table 1). Imaging at low vacuum (*LV*) with the directional backscattered electron detector (*DBS*). (B and C) Same protocol as in A but silver colloid mixed to the Epon combined with minimal resin embedding (protocol 06, Table 1). Imaging at low vacuum with the DBS (B) or at high vacuum (*HV*) with the T1 detector (*T1*) (C). While no charging is visible in the sample prepared according to protocol 01 (Table 1) at low vacuum (A), some regional charging (*arrowheads*) is detectable in samples prepared according to protocol 06 (Table 1), regardless of the vacuum mode and detector used. (*) bottom of the plastic dish. Scale bar = 5 µm.

samples prepared by our standard protocol [15] after on-section staining (not shown). Thin sections taken from the same block as used for block-face imaging were imaged by transmission electron microscopy (TEM) without on-section contrasting and demonstrated that heavy metal treatment produced no significant precipitates but excellent contrast (Supplementary Figure 5A).

The application of a second incubation step with osmium tetroxide after tannic acid treatment and *en bloc* treatment with lead aspartate (Table 1, protocol 09 to 11) resulted macroscopically and microscopically in the darkest cells (Note: here, we imaged the block-faces with inverted grayscale) of the protocols tested. However, contrast of major subcellular structures was lower than in the samples prepared without the second osmium tetroxide treatment (Figure 3). In general, the cytoplasm was very dense and, occasionally, organelles, such as mitochondria, appeared brighter than the surrounding cytoplasm (Figure 3C and D). Precipitates were visible around the cells but not within the cells which could be demonstrated by transmission electron

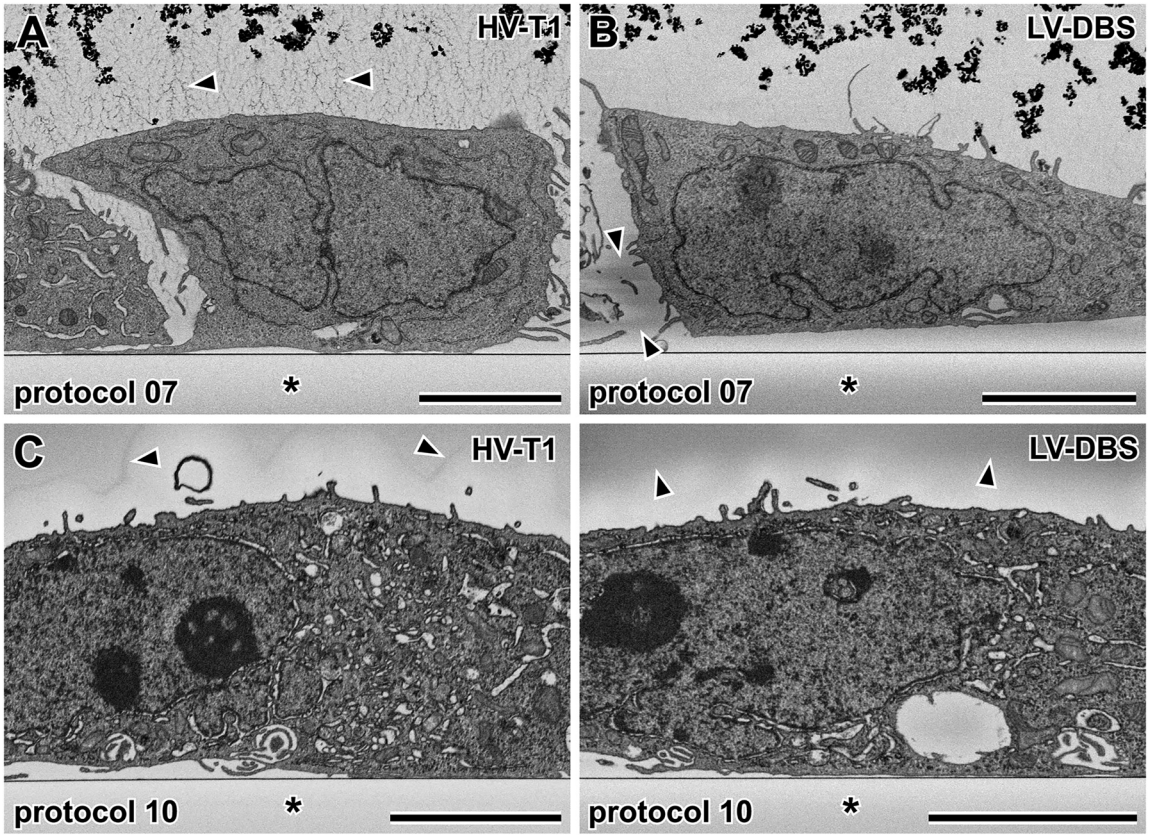

Figure 3: Block-face SEM of adherent HeLa cells in cross-section prepared with different protocols to increase heavy metal content of the sample. (A and B) Increased osmium tetroxide concentration and temperature of post-fixation (60 °C) plus *en bloc* contrasting with lead aspartate (protocol 07, Table 1). (C and D) Increased osmium tetroxide concentration and temperature of post-fixation (60 °C) plus a second osmium tetroxide incubation step after the tannic acid plus *en bloc* contrasting with lead aspartate (protocol 10, Table 1). Cells were embedded with the minimal embedding protocol (air blow variant) with (A and B) or without (C and D) the addition of silver colloid. Imaging was either performed at low vacuum (*LV*) with the directional backscattered electron detector (*DBS*) (A and C) or at high vacuum (*HV*) with the T1 detector (*T1*) (B and D). Moderate local charging of the block-face is visible in all of the images (*arrowheads*) but was restricted to the extracellular space. It is less pronounced in the images of samples prepared with a higher heavy metal content (C and D). The contrast of many structural details is sufficient in samples prepared with both protocols but is less pronounced in the samples prepared with the additional osmium tetroxide step. (*) bottom of the plastic dish. Scale bar = 5 µm.

microscopy of thin sections (Supplementary Figure 5B). The increased heavy metal deposition produced by the introduction of a second osmium tetroxide incubation step was clearly detectable in the thin sections and particular evident in an increased thickness of the membranes of the endoplasmic reticulum (Supplementary Figure 5B).

Samples from both modified protocol series (Table 1, protocol 07 to 08 and protocol 09 to 11) were tested by SBF SEM at low and at high vacuum conditions. SBF Imaging of samples prepared with a single osmium tetroxide incubation step, followed by tannic acid, uranyl acetate and lead aspartate (Table 1, protocol 07 and 08) was possible at both vacuum conditions using the respective detectors. However, at high vacuum and 50 nm section thickness, SBF imaging was only successful at low resolution (≥10 nm pixel size), because charging of the sample block introduced size and shape changes to imaged structures including the entire cell, which prevents a proper alignment of the image stack (Supplementary Video 4). Samples without silver colloid added to the Epon (Table 1, protocol 08) could hardly be serially imaged at high vacuum and, therefore, were not studied further. SBF SEM at low vacuum conditions was possible with a pixel size of 5 nm and above at a section thickness of 50 nm and at a contrast which allowed the visibility and recognition of major organelles and membrane systems (Figure 4A; Supplementary Videos 5–7). Constant imaging was possible at this resolution for several hundred sections with 50 nm thickness. For achieving lower z-resolution (i.e. thinner sections), the lateral resolution needed to be reduced to avoid softening of the surface resin layers by the concentrated beam. However, stable imaging series could be achieved at 8 and 10 nm pixel size with

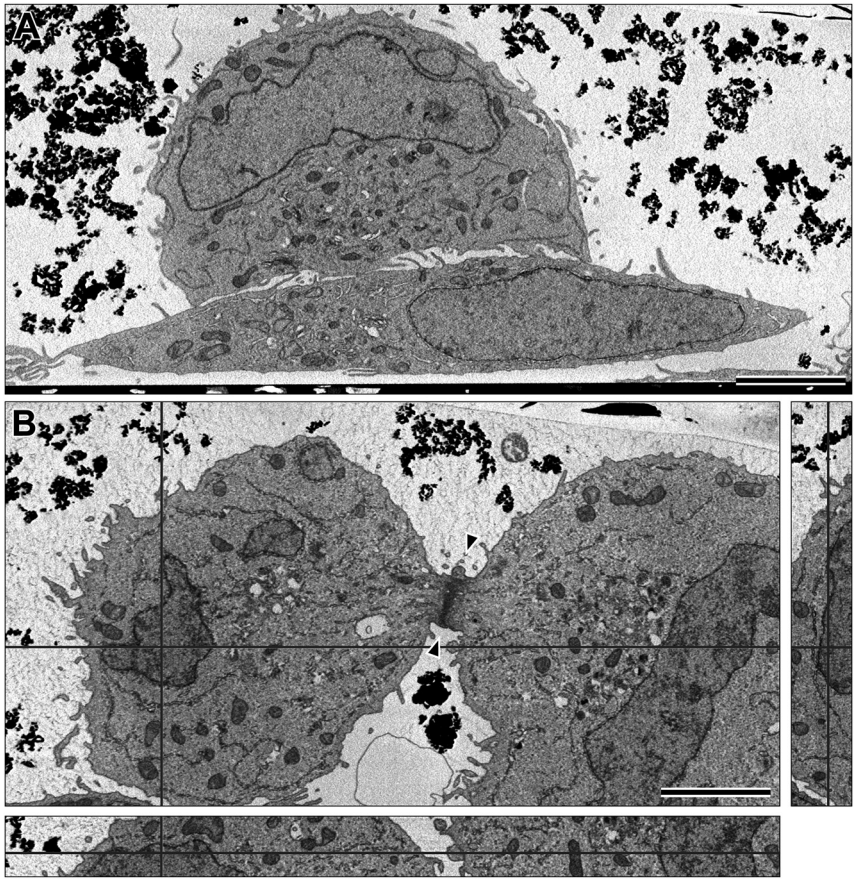

Figure 4: SBF SEM of adherent HeLa cells in cross-section prepared according to protocol 07 (Table 1). (A) Overview of two HeLa cells with clearly detectable subcellular organelles and structures (see also Supplementray Video 5). The image series was recorded at low vacuum with the DBS detector and at pixel size of 8 nm and a section thickness of 50 nm. (B) Orthogonal view of two dividing cells with a midbody (*arrowheads*) of a series recorded at isotropic resolution of 10 nm (image 133 of the series shown in Supplementary Video 6). Scale bar = 5 µm.

10 nm section thickness (Figure 4B; Supplementary Videos 5 and 7).

SBF SEM of samples prepared with an additional osmium tetroxide incubation step after tannic acid incubation (Table 1, protocol 09 to 11) allowed to set a slightly lower pixel size at both vacuum modes as compared with the protocols which applied only a single osmium tetroxide incubation step (Table 1, protocol 07). Samples without addition of silver colloid to the Epon were not evaluated by SBF imaging at high vacuum, because of the still significant charging, which allowed single scans of the block-face but no stable SBF imaging. At low vacuum conditions SBF imaging down to a pixel size of 3 nm at 50 nm section thickness could be achieved (Figure 5A; Supplementry Video 8). Minimal section thickness was 10 nm at 10 nm pixel size (Figure 5B; Supplementary Video 9) as with samples prepared only with one osmium tetroxide incubation step (Table 1, protocol 07). At high vacuum, SBF imaging was possible with a pixel size of 8 nm at 50 nm section thickness (Supplementary Video 10), which was better than with the samples that were prepared with only one osmium tetroxide incubation step. However, the final lateral structural resolution was lower than the actual pixel size achieved during imaging because of the reduced contrast of the samples in comparison to samples which were prepared with only one osmium tetroxide incubation step. We estimate the actual lateral structural resolution achieved with the two protocol variants to at least 10 nm because two closely apposed membranes, such as the inner membranes of mitochondria or the membranes of a thin tubule of the endoplasmic reticulum, were discernible if a gap of a single membrane width was visible between them (Figure 5A).

In summary, SBF SEM of adherent HeLa cells at low vacuum resulted in more stable image series at higher pixel and z-resolution than at high vacuum, regardless of the heavy metal load. And, the increased heavy metal load introduced by the additional osmium tetroxide incubation step (Table 1, protocol 09–11) allowed to set a slightly higher pixel

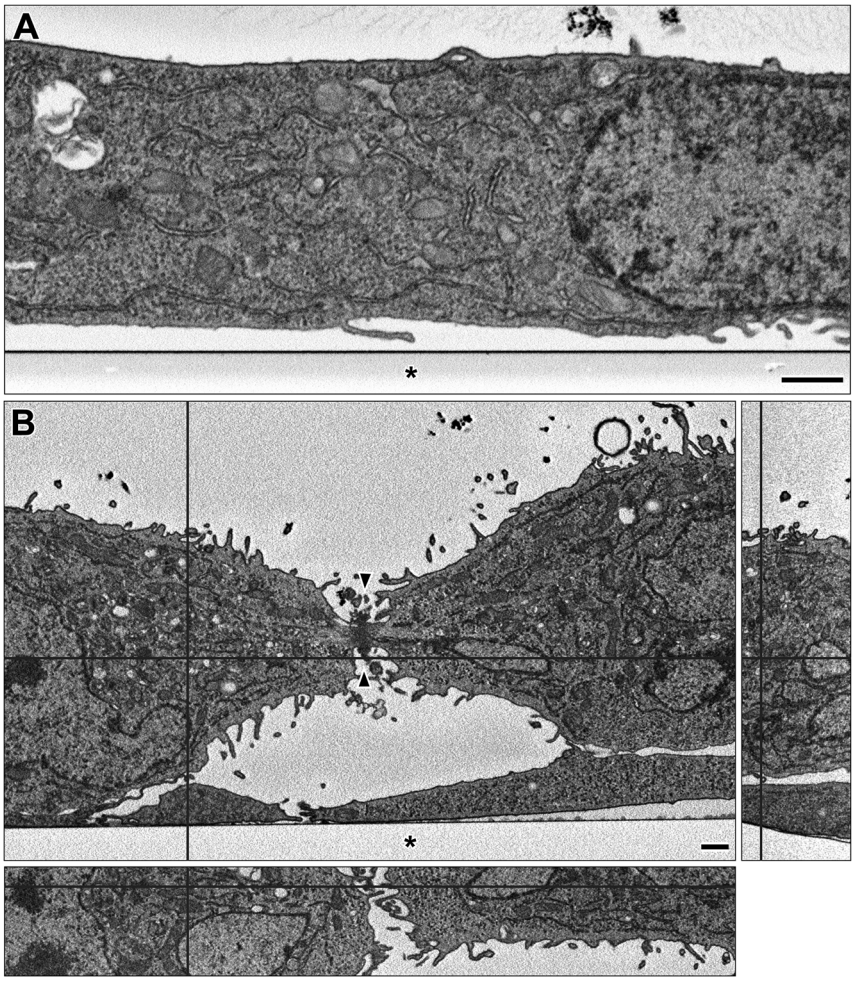

Figure 5: SBF SEM of adherent HeLa cells in cross-section prepared according to protocol 09 or 11 (Table 1). (A) Detail of a cell recorded at a pixel size of 3 nm and a section thickness of 50 nm using the DBS detector at low vacuum (protocol 09, Table 1). (B) Orthogonal view of two dividing cells with a midbody (*arrowheads*) of a series recorded at isotropic resolution of 10 nm (image 71 of the series shown in Supplementary Video 9) (protocol 11, Table 1). (*) bottom of the plastic dish. Scale bar = 1 µm.

resolution and provided better series stability at the cost of a lower contrast than the protocol that uses only one osmium tetroxide incubation step (Table 1, protocol 07 and 08).

4 Discussion

SBF SEM is a method which allows imaging of larger volumes of tissue, cells and small organs at low and medium EM resolution. It provides an alternative to the serial imaging of serial sections acquired by conventional ultramicrotomy and serial imaging by focussed ion beam (FIB) SEM (see [1] for a general overview and discussion of the various techniques). Due to the automated repetitive sectioning and imaging, the comparatively wide range of section thickness (approx. 10–500 nm) and maximal sample size (approx. 1 mm^2), SBF SEM is potentially able to achieve a reasonable throughput for the analysis of samples with a higher biological variability or samples from different experimental groups.

A higher throughput in SBF SEM requires optimized and standardized sample preparation protocols and workflows. Our study presents a method for SBF SEM of adherent cells cultivated in culture dishes with a thin plastic bottom which are widely used in cell biology. The entire preparation of cells was performed in the dishes without removing cells or plastic bottom. Mounting the embedded cells on their plastic support substrate for cross-sectioning by SBF SEM allowed to collect large series of images from many regions of the block-face in parallel while retaining the interface between cells and substrate. Remarkably, this was already possible by using a standard post-fixation and embedding protocol, which offered also to collect thin sections by

conventional ultramicrotomy for TEM analysis without compromise of the structural appearance.

Block-face imaging of cells on substrates, such as glass, metal or plastic, in cross-section is usually performed by FIB SEM, because the FIB is able to ablate any material at high z-resolution, which allows to achieve highest isotropic voxel resolution. However, speed of ablation is still slow and usually restricted to small areas and volumes although new plasma-milling techniques promise to solve this issue [24]. Our workflow for SBF SEM of cells on plastic substrate provides an alternative to the FIB SEM approach and allows voxel resolution of isotropic 10 nm or 3 nm at 50 nm section thickness with an approximal lateral structural resolution of 10 nm. The Volumescope allows SBF imaging down to 10 nm setting of section thickness at low vacuum in most samples, if the selected pixel size for imaging is around or higher than 10 nm and the beam conditions are selected in a way that the beam introduces only low energy into the block-face which avoids softening of the resin. Lower pixel size can be achieved in some samples without generally providing much more structural resolution. One reason for the high z-resolution (i.e. low section thickness) achieved by the Volumescope at low vacuum most probably is the efficient compensation of charges in the block-face. At high vacuum conditions the z-resolution of the SBF imaging is at least a factor 2 lower (i.e. a section thickness of 20 nm), even with high conductive samples.

SBF SEM of cells cultivated on plastic dishes was already performed by other groups, mainly to study correlative questions (e.g. [9,12]). However, in these studies sectioning was performed parallel to the plastic support and the plastic was either trimmed away or sectioned before reaching the cells. The advantage of this approach is that cells are oriented as in light or fluorescent microscopy and, since cultured cells are usually comparatively flat, fewer sections are required to record the entire volume of a cell than by taking cross-sections. A disadvantage is that the sectioned area is getting larger during sectioning which limits the depths of SBF imaging without further user intervention such as trimming. Our cross-section approach offers to section several hundred microns using the same block-face geometry. We did not test the upper limits of the approach but we think that even a block-face size above 1 mm length and block heights above 350 µm, which we have tested, are possible to section without trimming the sample block.

To increase contrast, resolution and image quality of the SBF imaging with our workflow, we increased the heavy metal content and applied modifications of the embedding, such as addition of silver colloids and reduction of resin layer thickness above cells (minimal embedding). The introduction of more heavy metals should not only provide more signal and contrast for backscattered electron imaging but also improve electrical conductivity of the sample [4]. Since cell cultures usually leave some gaps between cells, samples contain considerable volume of non-conductive resin. We tested, if we can render this volume more conductive by adding silver colloid as a filler to the Epon, which we have learned from the dissertation of Shami [6]. As expected, the more heavy metals we introduced, the more stable SBF imaging became and allowed to set a lower pixel size for imaging at higher resolution. Addition of the silver colloid filler also provided more stability for SBF imaging and was essential for imaging at high vacuum, but did not avoid charging completely. However, operation at low vacuum was the best choice in the Volumescope to achieve more stable SBF imaging at higher pixel resolution than at high vacuum.

Various protocols for introducing more heavy metals into samples for improving SBF imaging were published so far. Many of them used reduced osmium tetroxide, additional osmium tetroxide application after adding a linker or enhancer, and *en bloc* contrasting with uranyl acetate followed by lead aspartate (see [25]). An additional strategy reported is to increase the concentration and/or temperature of the heavy metal incubation (e.g. [26]). We also applied higher temperature and osmium tetroxide concentration which already improved the SBF imaging. The addition of lead aspartate *en bloc* treatment improved the imaging further and provided contrast and structural appearance which was very similar to TEM imaging of thin sections. The application of an additional osmium tetroxide incubation step most likely increased the heavy metal content of the samples further, because they appeared brighter (darker with reversed lookup table) than the samples without an additional osmium tetroxide step in backscattered electron imaging, but the contrast was generally lower or even locally reversed, as in the case of the mitochondria, most likely because of an overloading of the cytoplasm and membranes with heavy metals. In summary, the double application of osmium tetroxide provided better stability for imaging but at the cost of a rather unusual contrast. Further combinations of (heavy) metal treatment could be tested in future, such as the systematic application of UA-Zero or neodymium. If the silicone inserts are not used for processing, more combinations are possible, because these inserts interfere with some chemicals, e.g. the TCH.

In summary, our study provides a standard protocol and workflow for SBF SEM of adherent cells which seems to be generally applicable. Cells are cultivated in 35 mm dishes within small silicone inserts on thin plastic bottom which

requires only small volume of reagents. After primary fixation, a post-fixation protocol, which employs osmium tetroxide, tannic acid, uranyl acetate and lead citrate at 60 °C, is applied, which is very similar to most standard protocols for thin section electron microscopy and, thus, provide similar contrast and appearance of subcellular structures. Infiltration with Epon/acetone is performed in three steps, followed by removal of inserts and direct polymerization. After extraction of the samples from the dish, they were mounted upright on the stub for SBF SEM and were trimmed to the desired size. With the Teneo Volumescope, SBF imaging is best performed at low vacuum. Imaging at high vacuum, without any charge compensation, may need the addition of silver colloid to the Epon and/or the reduction of the Epon layer by using minimal embedding. Thin sections for TEM can be collected from the same blocks and visualized without further on-section staining to complement the volume imaging. The workflow offers many possibilities for adaptation to the requirements of other samples, microscopes and scientific questions.

Research ethics: Not applicable.

Author contributions: The authors have accepted responsibility for the entire content of this manuscript and approved its submission.

Competing interests: The authors state no conflict of interest.

Research funding: The study was supported by the German Research Foundation (DFG) Priority Programme SPP 2332 'Physics of Parasitism' (CK, TA).

Data availability: The raw data of image series shown in the video files are found on the Zenodo repository. Data set 01 – Raw and processed image series of Suppl. Video 1 (https://doi.org/10.5281/zenodo.11196419); Data set 02 – Raw and processed image series of Suppl. Video 2 https://doi.org/10.5281/zenodo.11197168; Data set 03 – Original ImarisFile used to generate Suppl. Video 3 https://doi.org/10.5281/zenodo.11198528; Data set 04 – Raw and processed image series of Suppl. Video 4 https://doi.org/10.5281/zenodo.11198586; Data set 05 – Raw and processed image series of Suppl. Video 5 https://doi.org/10.5281/zenodo.11198691; Data set 06 – Raw and processed image series of Suppl. Video 6 https://doi.org/10.5281/zenodo.11199320; Data set 07 – Raw and processed image series of Suppl. Video 7 https://doi.org/10.5281/zenodo.11199433; Data set 08 – Raw and processed image series of Suppl. Video 8 https://doi.org/10.5281/zenodo.11202406; Data set 09 – Raw and processed image series of Suppl. Video 9 https://doi.org/10.5281/zenodo.11203027; Data set 10 – Raw and processed image series of Suppl. Video 10 https://doi.org/10.5281/zenodo.11203782.

References

[1] C. J. Peddie, *et al*., "Volume electron microscopy," *Nat. Rev. Methods Primers*, vol. 2, p. 51, 2022.

[2] W. Denk and H. Horstmann, "Serial block-face scanning electron microscopy to reconstruct three-dimensional tissue nanostructure," *PLoS Biol.*, vol. 2, no. 11, p. e329, 2004.

[3] T. J. Deerinck, E. A. Bushong, M. H. Ellisman, and A. Thor, "Preparation of Biological Tissues for Serial Block Face Scanning Electron Microscopy (SBEM) V.2," *NCMIR*, 2022. https://doi.org/10.17504/protocols.io.36wgq7je5vk5/v2.

[4] S. Lippens, A. Kremer, P. Borghgraef, and C. J. Guérin, "Serial block face-scanning electron microscopy for volume electron microscopy," *Methods Cell Biol.*, vol. 152, pp. 69—85, 2019.

[5] B. Konopová and J. Týč, "Minimal resin embedding of SBF-SEM samples reduces charging and facilitates finding a surface-linked region of interest," *Front. Zool.*, vol. 20, no. 1, p. 29, 2023.

[6] G. J. Shami, "Probing the Unseen Depths of the Hepatic Microarchitecture via Multimodal Microscopy," Ph.D. dissertation, Univ. Sydney, Camperdown, NSW, AU, 2018, Available: http://hdl.handle.net/2123/20074.

[7] H. B. Nguyen, *et al*., "Conductive resins improve charging and resolution of acquired images in electron microscopic volume imaging," *Sci. Rep.*, vol. 6, 2016, Art. no. 23721.

[8] T. J. Deerinck, T. M. Shone, E. A. Bushong, R. Ramachandra, S. T. Peltier, and M. H. Ellisman, "High-performance serial block-face SEM of nonconductive biological samples enabled by focal gas injection-based charge compensation," *J. Microsc.*, vol. 270, no. 2, pp. 142—9, 2018.

[9] F. J. Flomm, *et al*., "Intermittent bulk release of human cytomegalovirus," *PLoS Pathog.*, vol. 18, no. 8, p. e1010575, 2022.

[10] L. Gerstenmaier, *et al*., "The autophagic machinery ensures nonlytic transmission of mycobacteria," *Proc. Natl. Acad. Sci. U. S. A.*, vol. 112, no. 7, pp. E687—92, 2015.

[11] K. Madela, S. Banhart, A. Zimmermann, J. Piesker, N. Bannert, and M. Laue, "A simple procedure to analyze positions of interest in infectious cell cultures by correlative light and electron microscopy," *Methods Cell Biol.*, vol. 124, pp. 93—110, 2014.

[12] M. S. Lucas, M. Günthert, A. G. Bittermann, A. de Marco, and R. Wepf, "Correlation of live-cell imaging with volume scanning electron microscopy," *Methods Cell Biol.*, vol. 140, pp. 123—48, 2017.

[13] C. Klotz, *et al*., "Highly contiguous genomes of human clinical isolates of Giardia duodenalis reveal assemblage- and sub-assemblage-specific presence-absence variation in protein-coding genes," *Microb. Genom.*, vol. 9, no. 3, p. mgen000963, 2023.

[14] J. Hahn, *et al*., "High sensitivity of giardia duodenalis to tetrahydrolipstatin (Orlistat) in vitro," *PLoS One*, vol. 8, no. 8, 2013, Art. no. e71597.

[15] M. Laue, "Chapter 1 — Electron microscopy of viruses," *Methods Cell Biol.*, vol. 96, pp. 1—20, 2010.

[16] J. Walton, "Lead asparate, an en bloc contrast stain particularly useful for ultrastructural enzymology," *J. Histochemi Cytochem.*, vol. 27, no. 10, pp. 1337—42, 1979.

[17] G. Wanner, *A Practical Guide to Scanning Electron Microscopy in the Biosciences*, Weinheim, Wiley-VCH, 2022.

[18] J. Schindelin, *et al*., "Fiji: an open-source platform for biological-image analysis," *Nat. Methods*, vol. 9, no. 7, pp. 676—82, 2012.

[19] I. Belevich, M. Joensuu, D. Kumar, H. Vihinen, and E. Jokitalo, "Microscopy Image Browser: A Platform for Segmentation and Analysis of Multidimensional Datasets," *PLoS Biol.*, vol. 14, no. 1, p. e1002340, 2016.
[20] K. D. Hagen, *et al*., "The domed architecture of Giardias ventral disc is necessary for attachment and host pathogenesis," *bioRxiv*, 2023. https://doi.org/10.1101/2023.07.02.547441.
[21] C. Nosala, *et al*., "Dynamic ventral disc contraction is necessary for Giardia attachment and host pathology," *bioRxiv*, 2023. https://doi.org/10.1101/2023.07.04.547600.
[22] R. D. Adam, "Giardia duodenalis: Biology and Pathogenesis," *Clin. Microbiol. Rev.*, vol. 34, no. 4, p. e0002419, 2021.
[23] C. Nosala, K. D. Hagen, and S. C. Dawson, "Disc-o-Fever': Getting Down with Giardia's Groovy Microtubule Organelle," *Trends Cell Biol.*, vol. 28, no. 2, pp. 99—112, 2018.
[24] M. Dumoux, *et al*., "Cryo-plasma FIB/SEM volume imaging of biological specimens," *Elife*, vol. 12, 2023, Art. no. e83623.
[25] B. M. Humbel, H. Schwarz, E. M. Tranfield, and R. A. Fleck, "Chemical Fixation," in *Biological Field Emission Scanning Electron Microscopy*, R. A. Fleck, and B. M. Humbel, Eds., Chichester, John Wiley & Sons Ltd, 2019, pp. 191—221.
[26] Y. Hua, P. Laserstein, and M. Helmstaedter, "Large-volume en-bloc staining for electron microscopy-based connectomics," *Nat. Commun.*, vol. 6, p. 7923, 2015.

Supplementary Material: This article contains supplementary material (https://doi.org/10.1515/mim-2024-0007).